iScience

CellPress
OPEN ACCESS

Article

The sequence of events of enteropathogenic *E. coli*'s type III secretion system translocon assembly

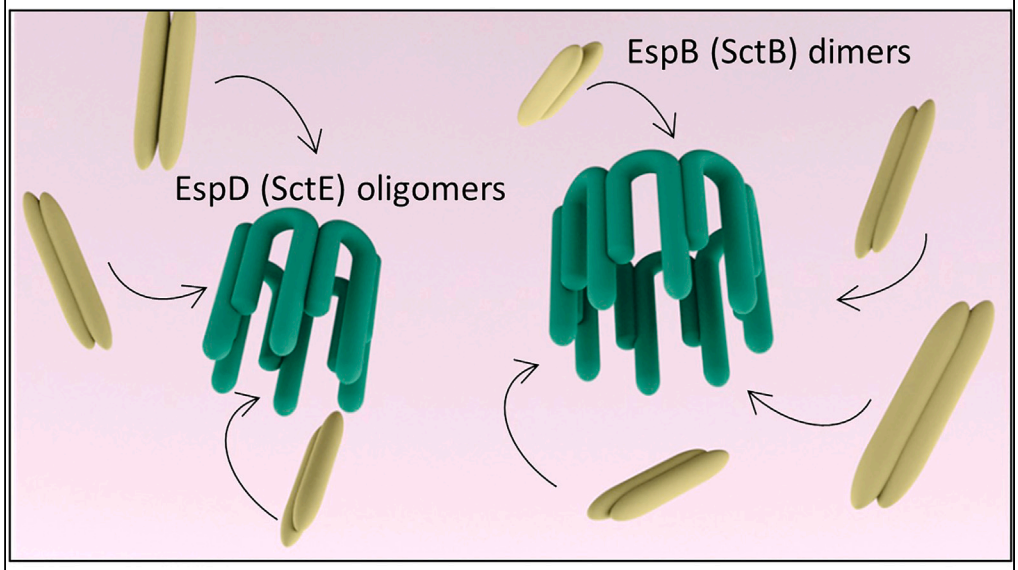

Jenia Gershberg, May Morhaim, Irina Rostrovsky, Jerry Eichler, Neta Sal-Man

salmanne@bgu.ac.il

Highlights

EspD (SctE) plays a dominant role in pore formation

EspD oligomerizes regardless of pH, membrane contact, or the presence of EspB (SctB)

EspB subunits integrate into the preformed EspD homo-oligomers

The transmembrane domain of EspB is involved in oligomerization

Gershberg et al., iScience 27, 109108
March 15, 2024
https://doi.org/10.1016/j.isci.2024.109108

iScience

CellPress
OPEN ACCESS

Article

The sequence of events of enteropathogenic *E. coli*'s type III secretion system translocon assembly

Jenia Gershberg,[1] May Morhaim,[1] Irina Rostrovsky,[1] Jerry Eichler,[2] and Neta Sal-Man[1,3,*]

SUMMARY

Many bacterial pathogens employ the type III secretion system (T3SS), a specialized complex that transports effector proteins that manipulate various cellular processes. The T3SS forms a translocon pore within the host-cell membrane consisting of two secreted proteins that transition from a soluble state into a transmembrane complex. Still, the exact sequence of events leading to the formation of a membranous functional pore remains uncertain. Here, we utilized the translocon proteins of enteropathogenic *E. coli* (EPEC) to investigate the sequence of those steps leading to translocon assembly, including self-oligomerization, hetero-oligomerization, interprotein interaction, and membrane insertion. We found that in EPEC, EspD (SctE) plays a dominant role in pore formation as it assembles into an oligomeric state, regardless of pH, membrane contact, or the presence of EspB (SctB). Subsequently, EspB subunits integrate into EspD homo-oligomers to create EspB-EspD hetero-oligomers that adopt a transmembrane orientation to create a functional pore complex.

INTRODUCTION

The type III secretion system (T3SS) is a crucial virulence machinery employed by many bacterial pathogens to transport effector proteins from the bacterial cytoplasm directly into host cells. These effector proteins manipulate various cellular processes to promote bacterial survival, replication, and colonization. The T3SS apparatus comprises a cytoplasmic ring, a basal body spanning the bacterial inner and outer membranes, an external needle (and sometimes a filament) extending from the bacterial surface to bridge the extracellular space, and a pore complex that is embedded within the host cell membrane, called the translocon.[1–5] The translocon pore is composed of SctB and SctE,[6–9] two hydrophobic proteins named according to the unified Sct (Secretion and Cellular Translocation) system.[4,10] These are attached to a third protein, called SctA, that forms the needle tip. These proteins (SctB, SctE, SctA), also referred to as translocators due to their role in effector translocation across the host membrane, must be secreted by the T3SS before reaching their extracellular T3SS complex positions. These translocators are secreted as intermediate T3SS substrates, namely, being secreted after the early substrates (needle and inner rod) proteins yet before the effector proteins.[4,11] Once in the extracellular environment, SctA forms a tip complex by homo-oligomerization that caps the distal end of the needle. SctB and SctE, on the other hand, hetero-oligomerize into a pore complex that creates the initial contact with the host membrane. This complex facilitates the translocation of effectors into the host cytoplasm.[6,12,13] Consequently, single null mutants of *sctA*, *sctB*, or *sctE* maintain standard type III secretion (T3S) ability, delivering substrates to the extracellular media, but cannot translocate effectors into host cells or cause disease in animal models.[14–19]

SctB and SctE belong to a unique group of proteins, called TMD-containing secreted proteins, that present seemingly conflicting features. On the one hand, they are secreted proteins that are found as soluble proteins, while, on the other hand, they harbor 1–2 transmembrane domains (TMDs) that promote their membrane integration. To prevent the integration of SctB and SctE into the bacterial membrane and allow for their secretion, their TMDs present a moderate level of hydrophobicity,[20] in addition to these proteins associating with class II T3SS chaperones. These chaperones prevent the premature folding of SctB and SctE and guide them to the sorting platform of the T3S apparatus. At the sorting platform, an ATPase enzyme (SctN) interacts with the chaperone-translocator complex, providing the energy necessary for chaperone release and subsequent secretion of the translocators through the T3SS channel.[21,22] The chaperone-binding domains (CBD) of most SctB and SctE proteins are located within the first 20-100 N-terminal residues.[23,24]

Once the proteins are secreted through the T3SS to the extracellular environment, they can remain soluble. It was proposed that the proteins undergo a transition from the soluble state into a transmembrane orientation upon reaching the host membrane. This transition is facilitated by the structural flexibility of SctB and SctE, shifting from a molten globule conformation in an aqueous solution to a ring-like structure composed of 6–8 subunits of each protein, embedded in the host membrane.[6,25–27] At present, the sequence of events that enable SctB and SctE to shift from the soluble state into the oligomeric membrane-embedded confirmation is unclear.

[1]The Shraga Segal Department of Microbiology, Immunology, and Genetics, Faculty of Health Sciences, Ben-Gurion University of the Negev, Beer Sheva, Israel
[2]Department of Life Sciences, Ben-Gurion University of the Negev, Beer Sheva, Israel
[3]Lead contact
*Correspondence: salmanne@bgu.ac.il
https://doi.org/10.1016/j.isci.2024.109108

In this study, we employed enteropathogenic *E. coli* (EPEC), a major cause of infantile diarrhea in developing countries,[28,29] to delineate the steps of translocon formation. The EPEC T3SS translocon comprises the proteins EspB (SctB) and EspD (SctE) encoded on the locus of enterocyte effacement (LEE) and correspond to 34 kDa (321 amino acid-long) and 39.5 kDa (380 amino acid-long) proteins, respectively. Here, we utilized purified EspB and EspD proteins to investigate the sequence of events leading to forming a functional pore.

RESULTS

$EspB_{wt}$-His is monomeric under soluble and membrane-simulating conditions

The T3SS translocon complex was shown to comprise multiple subunits of SctB and SctE proteins.[8,25,27,30–32] To investigate whether the EPEC SctB protein (EspB) oligomerizes on its own, we expressed EspB labeled with a His tag at its C-terminus ($EspB_{wt}$-His) in a EPEC Δ*espB* strain, grew the transformed strain under T3SS-induction conditions, and purified the protein from the culture medium (Figure 1A). The purified protein was then analyzed by size-exclusion chromatography (SEC) to determine its ability to form oligomers. Molecular weight standards served as protein size references and are presented at the top of the SEC profiles. The elution profile of purified $EspB_{wt}$-His under soluble conditions, as monitored by UV and recorded as a function of eluted volume, revealed the protein to mainly elute at an exclusion volume of 12–13 mL, corresponding to monomeric EspB (Figure 1B – upper panel). As oligomerization of T3SS translocators was previously suggested to occur only in the presence of detergent or upon interaction with model membranes,[27,30,33] we analyzed protein size in detergent (0.05% n-dodecyl-beta-maltoside; DDM). Under these conditions, $EspB_{wt}$-His was eluted earlier, with a peak at 10–11 mL, corresponding to molecular weight complexes larger than ~160 kDa ((Figure 1B – lower panel). To determine whether this size shift resulted from EspB oligomerization or elution of the protein in complex with DDM micelles, we analyzed this sample by SEC-MALS. Such analysis revealed that the protein eluted in complex with DDM micelles at a total size of 104 kDa (±6 kDa). Taking into consideration the size of a DDM micelle (66 kDa ±7.9 kDa[34]), the eluted protein thus corresponds to ~37 kDa (±3 kDa), which fits the size of monomeric EspB (Figure 1C). These results suggest that $EspB_{wt}$-His does not form oligomers in soluble conditions or the presence of micelles. Nonetheless, as we previously reported that $EspB_{wt}$-His was incapable of restoring the infectious ability of EPEC Δ*espB* strain toward host cells,[35] it remains plausible that this particular protein modification (i.e., tag introduction at the EspB C-terminus) does not allow for accurate reporting on EspB oligomerization.

We, therefore, created a new EspB construct where the His-tag was inserted into a permissive position at the 36th EspB protein residue,[7] generating $EspB^{36}$-His. We introduced the new construct into EPEC Δ*espB* and tested for restoration of effector translocation into host cells by the transformed strain. For this purpose, we infected HeLa cells with different EPEC strains (i.e., WT, Δ*espB*, and Δ*espB* expressing $EspB^{36}$-His) and evaluated the degradation pattern of c-Jun N-terminal kinase (JNK), a host protein that is cleaved by a translocated EPEC effector known as NleD.[36] As expected, WT EPEC induced extensive JNK degradation, relative to the uninfected HeLa cells and the same cells infected with the Δ*espB* mutant strain, which both showed no JNK degradation (Figure 2A). EPEC Δ*espB* that express $EspB^{36}$-His presented a similar JNK degradation pattern as WT EPEC bacteria, which indicated successful translocation of bacterial effectors into the host cells (Figure 2A). These results indicated that $EspB^{36}$-His is functional and can be employed to explore the oligomerization of the EspB protein. Accordingly, $EspB^{36}$-His protein was purified on a Ni-NTA resin and its size was analyzed under soluble (pH 7.0) and membrane-simulating conditions (in the presence of 0.05% DDM), using SEC. We also examined protein size in an acidic environment (pH 4.5), as previous reports indicated that such conditions facilitate the formation of T3SS translocator self- and hetero-oligomers.[27,33,37] We observed that $EspB^{36}$-His eluted at an exclusion volume of 14–15 mL, corresponding to the size of EspB dimer (~68 kDa), under soluble, either neutral or acidic, conditions (Figure 2B). A slightly larger complex eluted at an exclusion volume of 13–14 mL, corresponding to ~140 kDa, in the presence of detergent. This SEC shift can be attributed to the formation of a complex between a EspB dimer and a DDM micelle, which has a size of 66 kDa (±7.9 kDa). Our findings thus indicate that EspB forms a small-sized complex, potentially a dimer, rather than a larger oligomer comprising the complete set of subunits necessary for the mature EspB/EspD oligomer. To confirm that the elution profile of EspB was not affected by native EspD protein present in the supernatant during purification, we transformed the $EspB^{36}$-His expression vector into the EPEC Δ*espD* strain, which is compromised in terms of EspD secretion. Purification of $EspB^{36}$-His from the culture supernatant, followed by SEC analysis, revealed a comparable elution profile to that presented in Figure 2 (Figure S1). These results thus suggest that isolated EspB forms dimers.

EspD forms large oligomers under soluble conditions

To examine whether EspD (SctE), the major EPEC T3SS translocator, can self-oligomerize, we expressed a His-labeled variant ($EspD^{35}$-His) in the EPEC Δ*espD* strain. The transformed strain was shown to restore T3SS activity[35] and bacterial infectivity (Figure 3A), thus indicating that tag labeling at this position in EspD was permissive. The $EspD^{35}$-His protein was purified from the culture supernatant on a Ni-NTA resin column and analyzed by SEC to determine its ability to form large protein oligomers. SEC analysis of $EspD^{35}$-His revealed that the protein mainly eluted at an exclusion volume of 8 mL, corresponding to large molecular weight complexes (Figure 3B). Analysis of the eluted fractions by SDS-PAGE and western blotting with anti-EspD antibodies confirmed that the protein mainly eluted in the early fractions (8–9 mL), with noteworthy amounts in the 12 mL elution fraction (Figure 3B). To confirm that the early elution of EspD did not result from the formation of nonspecific-aggregates, we analyzed the Ni-NTA-purified $EspD^{35}$-His protein using an additional SEC column with higher resolution for large protein complexes (Superose 6 increase 10/300 GL). We observed a small elution peak that eluted near the void volume of the column (9.3 mL), likely corresponding to protein aggregates. However, the majority of the protein eluted as a polydisperse mixture with a peak at an exclusion volume of 17–18 mL, representing complexes around 160 kDa (Figure S2). These results suggest that EspD can form various large molecular weight oligomers under soluble conditions, prior to membrane contact and independently of EspB.

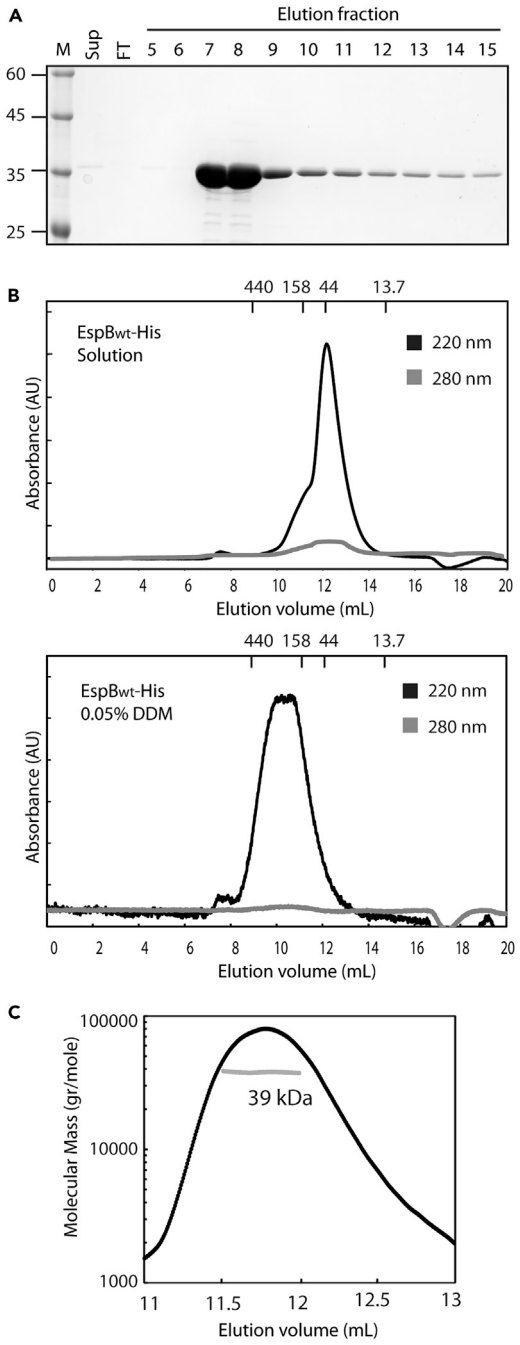

Figure 1. Oligomerization analysis of $EspB_{wt}$-His

(A) $EspB_{wt}$-His was purified from the culture supernatant of an EPEC Δ*espB* strain expressing $EspB_{wt}$-His by Ni-NTA column chromatography. Aliquots of the original bacterial supernatant (Sup), flow-through (FT), and eluted fractions were analyzed on SDS-PAGE and Coomassie staining. The molecular weight marker (M) is shown at the left of the gel.

(B) $EspB_{wt}$-His, purified on a Ni-NTA resin column, was subjected to SEC (Superose 12 10/300 GL). SEC analysis of $EspB_{wt}$-His under soluble conditions (upper panel) and in the presence of detergent (0.05% DDM; lower panel) was performed. UV profiles at 220 nm (black line, reflecting very low extinction coefficients) and 280 nm (gray line) are presented as a function of the eluted volume. $EspB_{wt}$-His eluted mainly as a monomeric protein (12–13 mL) under soluble conditions and as larger complexes (10–11 mL) under membrane-simulating conditions. Markers at the top of the SEC profile indicate the positions of the protein standards ferritin (440 kDa), aldolase (158 kDa), ovalbumin (44 kDa), ribonuclease (13.7 kDa).

(C) SEC (Superdex 200 10/30) - MALS analysis of $EspB_{wt}$-His protein in the presence of detergent (0.05% DDM) revealed a molecular weight of ~39 kDa (gray line), corresponding to a monomeric form of EspB.

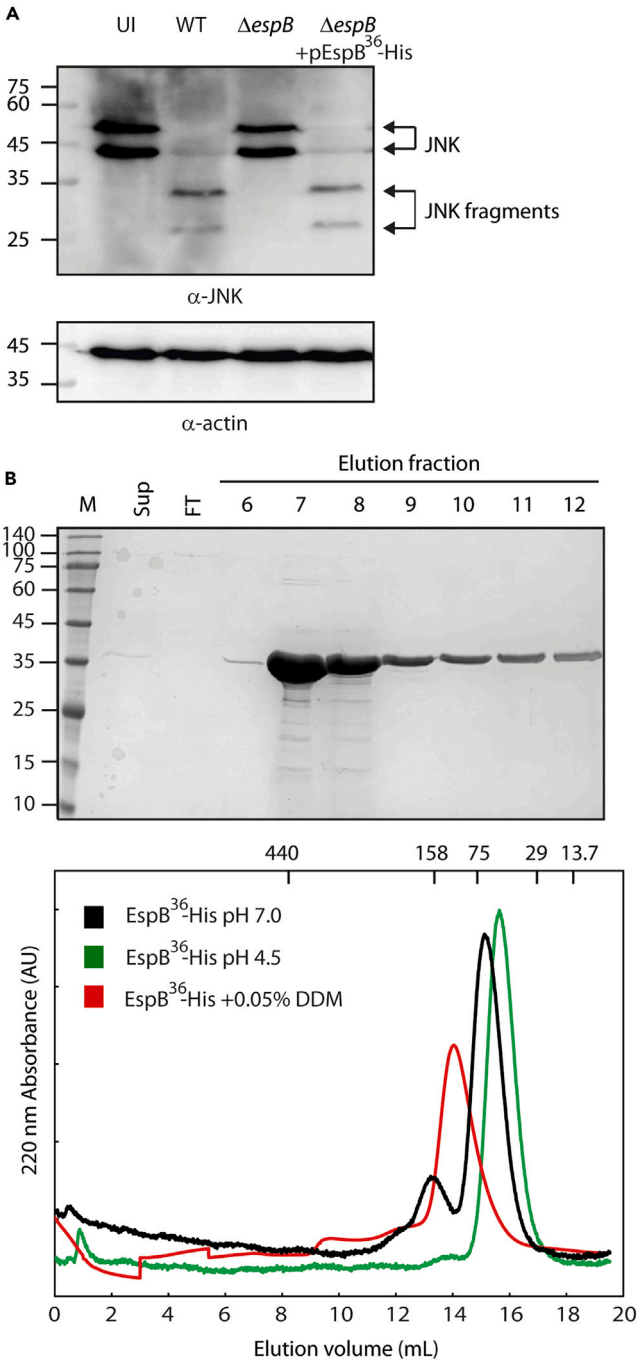

Figure 2. Oligomeric analysis of EspB^{36}-His

(A) Proteins extracted from HeLa cells infected with EPEC WT, Δ*espB*, and Δ*espB* expressing EspB^{36}-His. Aliquots were subjected to western blot analysis using anti-JNK and anti-actin (loading control) antibodies. JNK and its degradation products are indicated at the right of the gel. A sample of uninfected (UI) cells served as negative control.

(B) EspB^{36}-His was purified from the culture supernatant of EPEC Δ*espB* bacteria expressing EspB^{36}-His grown under T3SS-inducing conditions by Ni-NTA column chromatography. Aliquots of the original bacterial supernatant (Sup), flow-through (FT), and eluted fractions were analyzed by SDS-PAGE and Coomassie staining (upper panel). Molecular weight markers (M) are shown at the left of the gel. Purified EspB^{36}-His (fraction 7) was subjected to SEC (Superdex 200 10/300 GL), and monitored at a wavelength of 220 nm to follow protein elution (lower panel). SEC analyses of EspB^{36}-His in soluble natural conditions (black), acidic conditions (green), and in the presence of detergent (red) were performed by monitoring UV as a function of the eluted volume. Markers at the top of the SEC profile indicate the positions of the standards: Ferritin (440 kDa); Aldolase (158 kDa); Conalbumin (75 kDa); Carbonic Anhydrase (29 kDa); and Ribonuclease (13.7 kDa).

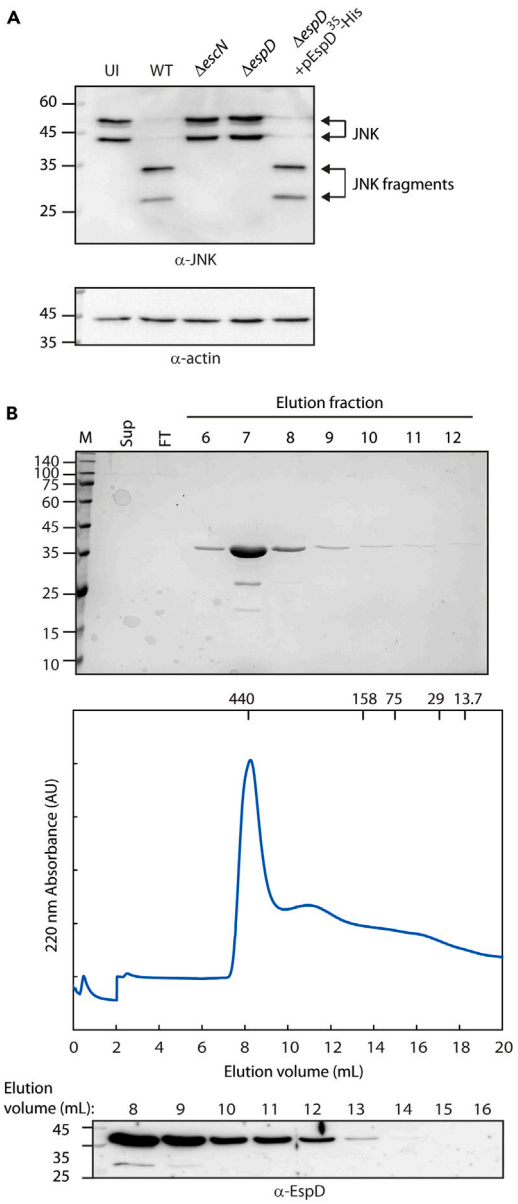

Figure 3. SEC analysis of purified EspD^{35}-His

(A) Proteins extracted from HeLa cells infected with EPEC WT, Δ*escN*, Δ*espD, and* Δ*espD* expressing EspD^{35}-His. The samples were subjected to western blot analysis using anti-JNK and anti-actin (loading control) antibodies. JNK and its degradation products are indicated at the right of the gel. A sample of uninfected (UI) cells served as a negative control.

(B) EspD^{35}-His was purified from the culture supernatant of EPEC Δ*espD* bacteria expressing EspD^{35}-His grown under T3SS-inducing conditions by Ni-NTA column chromatography. Aliquots of the original bacterial supernatant (Sup), flow-through (FT), and eluted fractions were analyzed by SDS-PAGE and Coomassie staining (upper panel). Molecular weight markers (M) are shown at the left of the gel. Purified EspD^{35}-His (fraction 7) was subjected to SEC (Superdex 200 10/300 GL) under soluble natural conditions to follow protein elution by monitoring UV wavelength of 220 nm as a function of the eluted volume (mL). Markers at the top of the SEC profile indicate the positions of the standards as described in the legend to Figure 2. Lower panel: eluted fraction samples separated by SDS-PAGE and analyzed by western blotting with an anti-EspD antibody.

EspB integrates into the EspD oligomer

To evaluate whether EspB subunits can incorporate into the EspD oligomer, we mixed purified EspB^{36}-His with EspD^{35}-His under soluble conditions at a 1:1 molar ratio and analyzed the SEC elution profile. We observed two protein elution peaks, one at an exclusion volume of 8–9 mL, corresponding to large protein complexes, and another at 14–15 mL, corresponding to homo- or hetero-dimers (Figure 4). Since the SEC profile was uninformative regarding the identity of the proteins in each peak, we analyzed the SEC eluted fractions by western

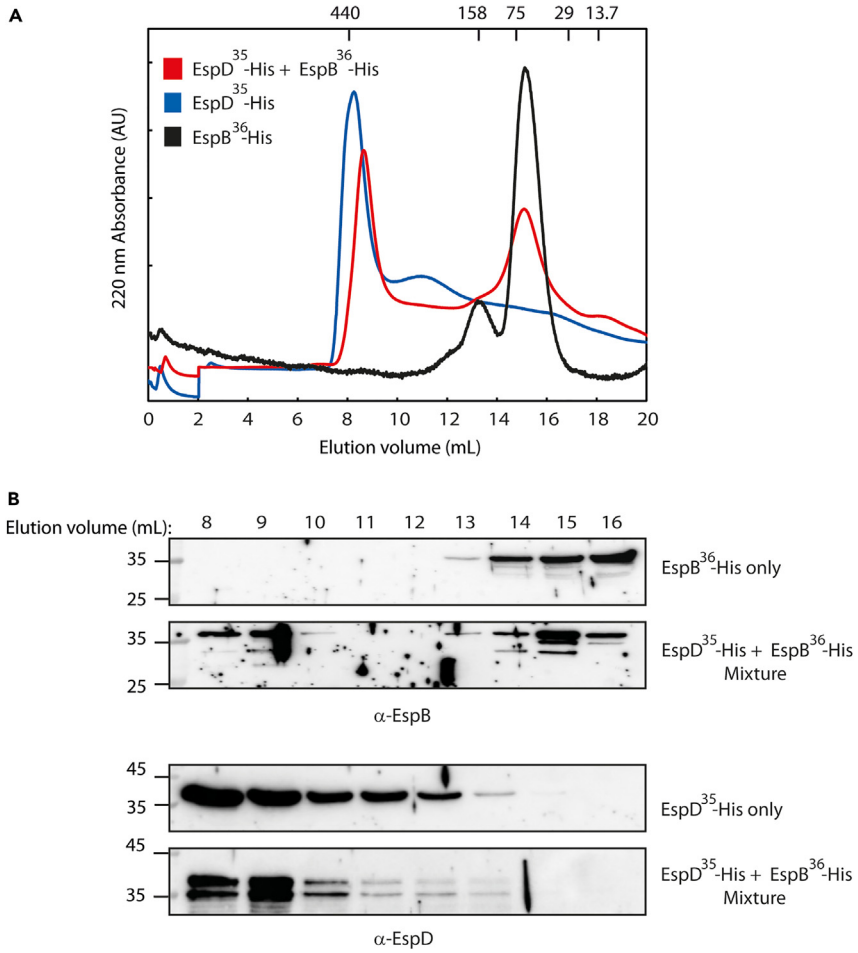

Figure 4. EspB^{36}-His integrates into the EspD^{35}-His oligomer

(A) Purified EspB^{36}-His and EspD^{35}-His were mixed under soluble natural conditions at a 1:1 ratio and subjected to SEC analysis (Superdex 200 10/300 GL) to monitor oligomeric state. SEC analyses of EspB^{36}-His alone (black), EspD^{35}-His alone (blue), and the mixture of the two proteins (red) were performed and presented as UV as a function of the eluted volume (mL). Markers at the top of the SEC profile indicate the positions of the standards as described in the legend to Figure 2.

(B) Samples of the elution fractions were separated by SDS-PAGE and analyzed by western blotting with anti-EspB and anti-EspD antibodies.

blotting with anti-EspB and anti-EspD antibodies. We observed that while EspD^{35}-His mainly eluted at fraction 8–9 mL, regardless of EspB^{36}-His presence, the elution profile of EspB^{36}-His was shifted to larger complexes in the presence of EspD^{35}-His (Figure 4). These results suggested that EspB^{36}-His can incorporate into the EspD^{35}-His oligomer following EspD self-oligomerization to later form a functional hetero-oligomeric pore.

Expression of EspB^{36}-His and EspD^{35}-His restore pore-forming activity of Δ*espB* and Δ*espD* bacteria, respectively

To determine whether EspB^{36}-His and EspD^{35}-His are functional, we examined their abilities to complement the deficiency of EPEC Δ*espB* and EPEC Δ*espD* strains to form pores within the host cell membrane. To quantify pore formation, we monitored the uptake of the cell-impermeant dye, propidium iodide (PI), which enters cells through plasma membrane pores.[38,39] We observed that HeLa cells infected with WT EPEC showed high levels of PI uptake, as compared to uninfected cells or cells infected with the EPEC Δ*escN* mutant strain (Figure 5). The Δ*escN* strain is deleted of the T3SS ATPase-encoding gene and, therefore, cannot secrete the translocon proteins (and T3SS effectors) needed to form functional translocon pores.[40] As expected, both the EPEC Δ*espB* and Δ*espD* strains showed low levels of PI uptake, indicating that both EspB and EspD are required for pore formation in the host cell membrane (Figure 5). EPEC Δ*espB* expressing EspB^{36}-His and EPEC Δ*espD* expressing EspD^{35}-His showed significantly higher PI uptake, as compared to their background strains (Figure 5). These results indicated that the recombinant EspB^{36}-His and EspD^{35}-His constructs respectively complemented, at least partially, EPEC Δ*espB* and EPEC Δ*espD* deficiencies in pore formation. EPEC Δ*espB* and Δ*espD* strains that express the non-tagged EspB and EspD proteins, respectively, showed PI uptake similar to EPEC WT (Figure S3), suggesting that His-labeling of EspB and EspD, even at inter-protein positions, slightly

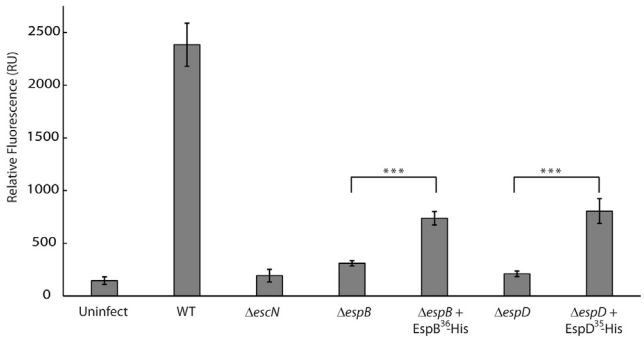

Figure 5. EspB^{36}-His and EspD^{35}-His respectively restore the pore-forming activity of Δ*espB* and Δ*espD* bacterial strains

HeLa cells were infected with pre-activated EPEC WT, Δ*escN*, Δ*espB*, Δ*espD*, Δ*espB* expressing EspB^{36}-His and Δ*espD* expressing EspD^{35}-His for 1.5 h. The infected cells were washed, incubated with PI for 2 min, re-washed, and fixed. The amount of PI in the cells was determined using a TECAN plate reader (excitation at 533 nm and emission at 620 nm) and presented as relative units (RU). Bars represent the geometric mean of five repeats for each strain from a representative experiment. Error bars represent standard deviation. Statistical significance was determined by Student's *t* test (***, $p < 0.005$).

interfered with their ability to form pores. In addition, a sample comprising a mixture of the EPEC Δ*espB* expressing EspB^{36}-His and EPEC Δ*espD* expressing EspD^{35}-His strains completely restored the pore-forming activity of the null strains to the level observed with WT EPEC (Figure S3). Such complementation can likely be attributed to the appropriate stoichiometric ratio between the two over-expressed secreted proteins. Note that PI uptake by HeLa cells infected with the two complemented strains (EPEC Δ*espB* + EspB^{36}-His and EPEC Δ*espD* + EspD^{35}-His) was much lower than that shown by HeLa cells infected with WT EPEC. In contrast, the complemented strains showed similar effector translocation ability as the WT strain (Figures 2 and 3). These results suggest that bacterial infectivity, measured by the activity of translocated effectors into the cell host, is not directly associated with the number of functional pores.

The TMD of EspB is involved in oligomerization

We previously found that alteration of the EspB TMD by introducing alternative hydrophobic sequences allowed for proper EspB secretion but impaired its translocation into the host membrane and, consequently, that of EspD, as well as of Tir, the first and the most abundant T3SS effector.[35] However, the precise mechanism underlying this impairment remained elusive. Here, we investigated whether EspB with altered TMD sequences lost its translocation-mediating ability due to disruption of EspB-EspD oligomerization. Accordingly, we cloned two TMD-exchanged versions of the EspB^{36}-His construct. The TMD sequence of EspB was replaced by either of the two Tir TMDs. As Tir belongs to the TMD-containing secreted protein group, together with EspB and EspD, these TMD sequences should support protein secretion. EspB^{36}-His Tir1 was generated by replacing the 16 core residues of the EspB TMD with the corresponding sequence from the N-terminal TMD sequence of Tir and EspB^{36}-His Tir2, by replacement with the C-terminal Tir TMD. The two TMD-exchanged EspB constructs (pEspB^{36}-His Tir1 and pEspB^{36}-His Tir2) were transformed into the EPEC Δ*espB* strain, and their expression and secretion were confirmed (Figure 6A). The proteins were then purified from the culture supernatant on Ni-NTA resin. Circular dichroism (CD) spectra measured for EspB^{36}-His indicated the presence of a helical structure, with minima of nearly equal intensity at 222 and 208 nm (Figure S4). The CD spectra of the TMD-exchanged EspB variants, Tir1 and Tir2, also indicated helical structure, although their spectra showed increased intensity at the 208 nm minimum, relative to the ellipticity at 222 nm (Figure S4). These results suggest the TMD-exchanged EspB variants adopted an overall similar folding, although not identical, to the original EspB protein. We analyzed the proteins in terms of their oligomeric status by subjecting them to SEC. Unexpectedly, we observed that both EspB^{36}-His Tir1 and EspB^{36}-His Tir2 displayed distinct elution profiles, as compared to EspB^{36}-His. While EspB^{36}-His eluted as a dimer (at an exclusion volume of ~14–15 mL), EspB^{36}-His Tir1 and EspB^{36}-His Tir2 presented continuous elution profiles with a prominent peak at an exclusion volume of 8–9 mL, corresponding to large oligomeric complexes (~440 kDa) (Figure 6B). Analysis of the eluted fractions by SDS-PAGE and western blot analysis using anti-EspB antibodies showed that EspB^{36}-His mainly eluted in fractions corresponding to the size of a dimer (Figure 6C). In contrast, the TMD-exchanged EspB variants were detected throughout the elution profile with a subtle peak at the early elution volumes, which was more pronounced in the analysis of the EspB^{36}-His Tir1 protein (Figure 6C). These results suggested that replacement of the EspB TMD sequence with the Tir1 or Tir2 TMD altered global EspB organization, which might have disrupted the ability of EspB subunits to integrate into oligomeric EspD to form functional EspB-EspD complexes.

Impaired oligomerization of EspB disrupts pore formation and hampers host cell infection

To determine whether the modified oligomeric arrangements of TMD-exchanged versions of EspB led to a decreased ability to translocate effectors into host cells, we infected HeLa cells with EPEC Δ*espB* expressing EspB^{36}-His, EspB^{36}-His Tir1 or EspB^{36}-His Tir2 and examined the cleavage pattern of JNK. Our results indicated that in contrast to the EspB^{36}-His-transformed strain, which complemented the inability of Δ*espB* cells to translocate effectors into host cells and to degrade cellular JNK, EspB^{36}-His Tir1 and EspB^{36}-His Tir2 were unable to complement this deficiency (Figure 7A). In addition, bacterial pore formation analysis also showed that Δ*espB* expressing either EspB^{36}-His Tir1 or EspB^{36}-His Tir2 exhibited

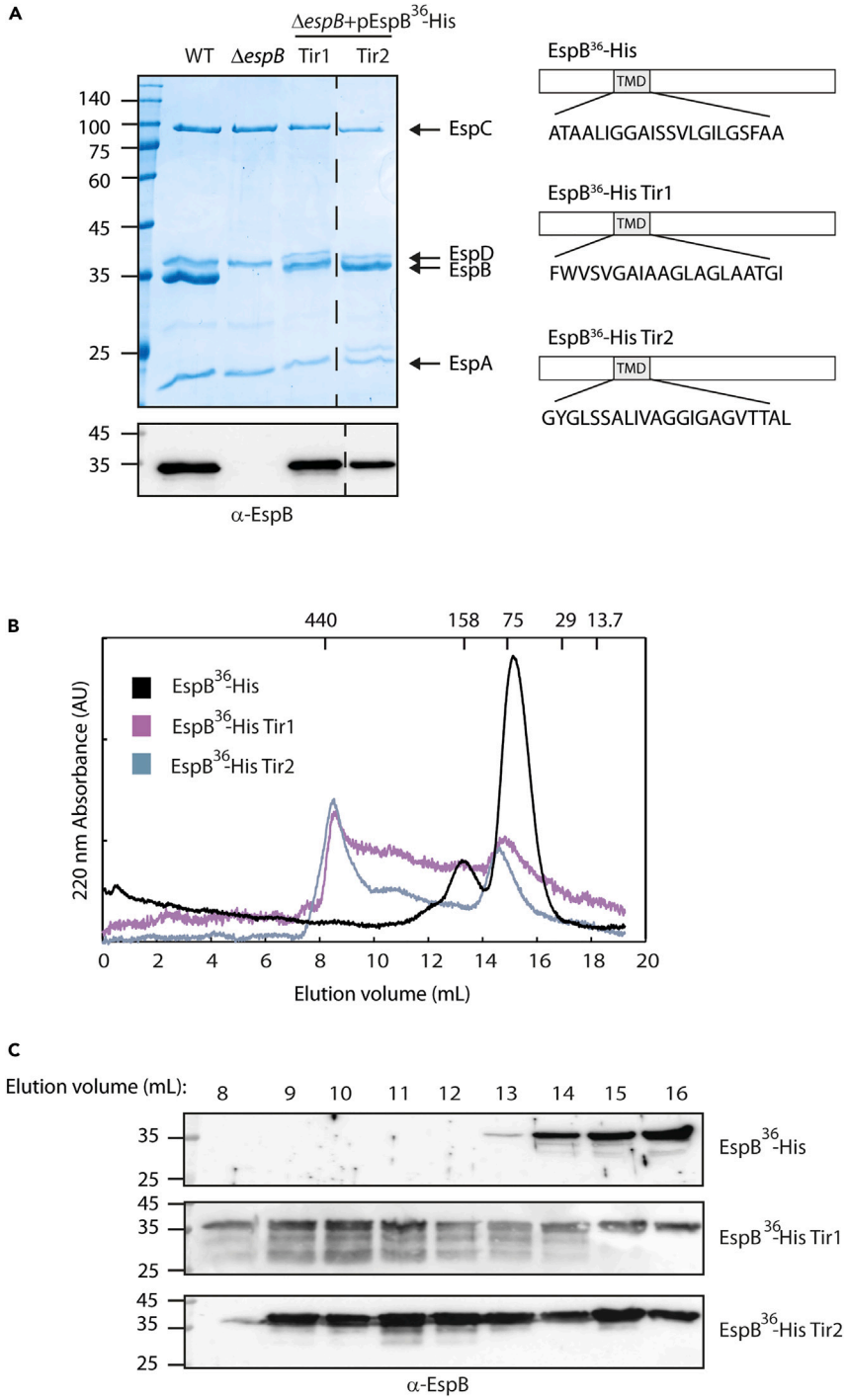

Figure 6. SEC analysis of TMD-exchanged EspB proteins

(A) EPEC Δ*espB* expressing EspB^{36}-His, EspB^{36}-His Tir1, or EspB^{36}-His Tir2 were grown under T3SS-inducing conditions. Bacterial supernatants and pellets were separated, normalized, and analyzed via 12% SDS-PAGE with Coomassie staining (top panel) or western blotting analysis using an anti-EspB antibody (bottom panel). The positions of the T3SS-secreted translocators EspA, EspB, and EspD are marked on the right of the gel. The location of EspC, which is not secreted by the T3SS, is also marked. Schemes of the EspB^{36}-His, EspB^{36}-His Tir1, and EspB^{36}-His Tir2 proteins, with their corresponding TMD sequences highlighted, are presented. The minor deviation in the position of EspB on the Coomassie gel can be attributed to an uneven run, as corroborated by a corresponding shift in the position of the EspA protein.

Figure 6. *Continued*

(B) EspB^{36}-His Tir1 and EspB^{36}-His Tir2 were collected and purified using Ni-NTA. The proteins (EspB^{36}-His, EspB^{36}-His Tir1, and EspB^{36}-His Tir2) were subjected to SEC (Superdex 200 10/300 GL). SEC analyses of EspB^{36}-His (black), EspB^{36}-His Tir1 (purple), and EspB^{36}-His Tir2 (gray) were performed by monitoring UV as a function of the eluted volume (mL). Markers at the top of the SEC profile indicate the positions of the standards as described in the legend to Figure 2.

(C) Aliquots of elution fractions were separated by SDS-PAGE and analyzed by western blotting with an anti-EspB antibody.

lower PI uptake and reduced pore formation activity than EspB^{36}-His (Figure 7B). To examine the ability of EspB^{36}-His Tir1 and EspB^{36}-His Tir2 expression to induce a dominant negative response and disrupt bacterial infection, we expressed EspB^{36}-His Tir1 and EspB^{36}-His Tir2 in the WT EPEC strain and examined host cell infectivity. We found that these strains generated a similar JNK degradation pattern as seen with WT EPEC cells, thus suggesting that the expression of non-functional EspB proteins did not have a dominant-negative effect (Figure 7A). Examination of the pore-forming ability of WT EPEC strain expressing EspB^{36}-His showed enhanced PI intake, as compared to WT EPEC bacteria (Figure 7B). WT EPEC expressing EspB^{36}-His Tir1 or EspB^{36}-His Tir2, however, showed reduced pore-forming activities, as compared to the WT EPEC strain expressing EspB^{36}-His (Figure 7B). These results suggest that TMD-exchanged EspB variants present dysfunctional translocation activity due to compromised oligomerization and that, while no dominant-negative effect was observed in the effector translocation assay, a partial effect on pore-forming activity was demonstrated.

DISCUSSION

The formation of a functional pore within the host cell membrane represents the final step in the T3SS assembly before translocation of effector proteins into the host cell. Despite its crucial role in bacterial infection, the specific sequence of events leading to pore formation remains unresolved. Although it was established that assembly of the translocon involves the formation of a hetero-oligomeric ring complex comprising the minor (EspB/SctB) and major translocon (EspD/SctE) proteins within the host membrane, the precise order of the individual steps leading to pore formation remains elusive. While it is known that the construction of the pore initiates with the secretion of these two translocon proteins into the extracellular medium,[19,41,42] the sequential order of subsequent steps, including self-oligomerization, hetero-oligomerization, interprotein interaction, acquisition of transmembrane orientation, and execution of translocon function within the host membrane, are still not known. In this study, we sought to determine the sequence of events leading to the formation of the EPEC T3SS translocon.

To determine whether EspB can individually self-oligomerize, we purified EspB presenting a His-tag at its C-terminus (EspB$_{wt}$-His) and analyzed its ability to form high molecular weight complexes. SEC analysis indicated that the protein elutes as a monomer under soluble, acidic, and membrane-simulating conditions (Figure 1). These results oppose previous reports showing that PopD (SctB) from *Pseudomonas aeruginosa* forms oligomeric pores in model membranes both individually and in combination with PopB (StcE).[32,43] Nevertheless, it is possible that our findings can be attributed to the addition of the His-tag at the protein C-terminus, a modification which was shown to disrupt EspB function in that EspB$_{wt}$-His was unable to complement the translocation activity of the EPEC Δ*espB* strain.[35] To examine the self-oligomerization of functional EspB, we inserted a histidine tag at position 36 (EspB^{36}-His), a position that tolerates alteration (Figure 2A;[7]). We determined that EspB^{36}-His runs as a dimer in natural, acidic, and membrane-simulating conditions. We, therefore, concluded that EspB does not form multi-subunit oligomers independently. Instead, we revealed that EspD forms high molecular weight oligomers regardless of pH, membrane contact, or the presence of EspB (Figure 3). Furthermore, we found that EspB subunits can integrate into these pre-existing EspD oligomers (Figure 4). This result highlights the intricate interplay between EspB and EspD, suggesting EspD to play a dominant role in inducing the oligomerization required for the translocon assembly. These findings, moreover, agree with our previous observation that EspD was translocated into membranes of cells infected with a mutant EPEC strain devoid of *espB*,[35] thus indicating that EspD translocation is independent of EspB. In addition, our results are supported by reports showing that stable integration of the minor translocon protein (SctB) is dependent on the initial integration of the major translocon protein (SctE),[44–46] as well as work showing that a *Yersinia* spp. *yopB* (SctE) mutant did not generate channels, while a mutant devoid of *yopD* (SctB) presented current fluctuations that differed from those observed with wild-type bacteria.[47] Together, our results, along with those from these previous studies, suggest that the self-oligomerization of EspD occurs prior to EspD-EspB hetero-oligomerization.

The two translocon proteins belong to a unique group of secreted proteins that contain TMDs. These regions include the highest level of sequence identity among the translocon proteins.[48] We have previously shown that replacement of these TMDs, even by TMDs from other TMD-containing secreted proteins, impairs post-secretion function of these translocon components and prevents the formation of functional pores.[35] Here, we considered whether the EspB TMD-exchanged variants were defective in terms of their ability to dimerize and integrate into EspD oligomers. Unexpectedly, we found that EspB^{36}-His Tir1 and EspB^{36}-His Tir2 demonstrated enhanced oligomerization and formation of high-molecular weight complexes (Figure 6). We hypothesize that such oligomeric organization of EspB^{36}-His Tir1 and EspB^{36}-His Tir2 prevents the ability of individual subunits to integrate into the EspD oligomer and form hetero-oligomers. In light of previous results showing that EspB Tir1 and EspB Tir2 cannot translocate into host cell membranes,[35] we deduced that EspB-EspD hetero-oligomer formation occurs prior to host cell membrane integration. Consequently, EPEC Δ*espB* bacteria expressing EspB^{36}-His Tir1 or EspB^{36}-His Tir2 were impaired for translocon formation and abrogated effector translocation (Figure 7). These results correlate with our results showing only a mild dominance-negative effect in a WT EPEC strain expressing either EspB^{36}-His Tir1 or EspB^{36}-His Tir2 (Figure 7A), thus indicating that the presence of TMD-exchanged versions of EspB does not dramatically interfere with the native EspB protein due to limited integration into the translocon pore.

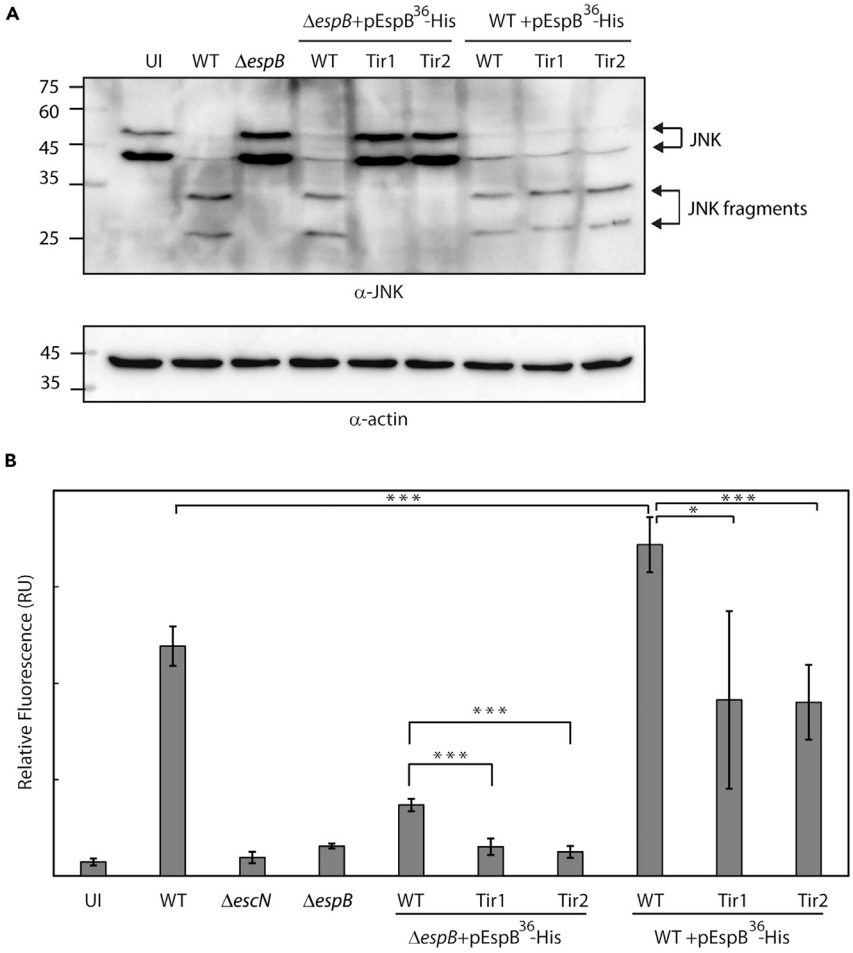

Figure 7. Effector translocation and pore-forming activity of EspB^{36}-His Tir1 and EspB^{36}-His Tir2

(A) Protein extracted from HeLa cells infected with pre-activated EPEC WT, Δ*escN*, Δ*espB*, Δ*espB* expressing EspB^{36}-His, EspB^{36}-His Tir1 or EspB^{36}-His Tir2 were subjected to western blot analysis using anti-JNK and anti-actin (loading control) antibodies. To examine the dominant-negative effect of TMD-exchanged EspB variant expression on EPEC WT infectivity, we extracted proteins from HeLa cells infected with WT EPEC expressing EspB^{36}-His, EspB^{36}-His Tir1, or EspB^{36}-His Tir2. The positions of JNK and its degradation products are indicated on the right of the gel. A sample of uninfected (UI) cells served as a negative control.

(B) HeLa cells were infected with the strains described in panel A for 1.5 h, washed, incubated with PI for 2 min, re-washed, and fixed. The amount of PI in the infected cells was determined using a TECAN plate reader (excitation at 533 nm and emission at 620 nm) and presented as relative units (RU). Bars represent the geometric mean of five repeats for each strain from a representative experiment. Error bars represent standard deviation. Statistical significance was determined by Student's *t* test (*, $p < 0.05$; ***, $p < 0.005$).

In conclusion, our findings indicate that EspD, which is secreted adjacent to sites of T3SS complex assembly, undergoes self-oligomerization, resulting in the formation of a complex that serves as the scaffold for the integration of EspB subunits. This hetero-oligomer can then insert into the host cell membrane to create a pore complex that translocates various effector proteins into the host cytoplasm (as suggested by the schematic model presented in Figure 8). Further research into the intricate interplay between these crucial elements, as well as their interactions with the T3SS filaments (formed by the EspA protein), could provide novel targets to block the initial steps of pathogen-host interactions, opening avenues for potential intervention strategies.

STAR★METHODS

Detailed methods are provided in the online version of this paper and include the following:

- KEY RESOURCES TABLE
- RESOURCE AVAILABILITY
  - Lead contact
  - Materials availability
  - Data and code availability

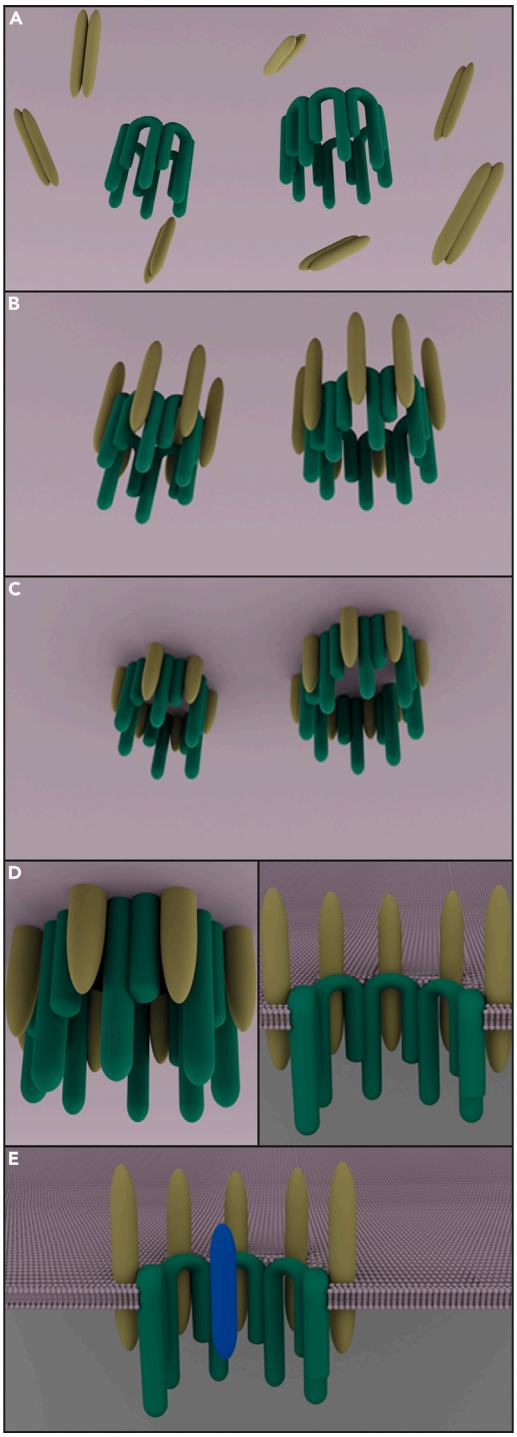

Figure 8. Schematic model of the chronological sequence of events of EPEC translocon formation

(A) EspD (dark green) forms homo-oligomers, while EspB (light green) is found as dimers.

(B) EspB binds EspD and integrates into the EspD homo-oligomers.

(C) The resulting hetero-oligomers integrate into the host cell membrane and create pore complexes (D – bottom view [left panel] and cross-sectional view [right panel]) that allows the passage of effector proteins into the host cytoplasm (E). The model presents a simplified representation that excludes extra T3SS components (such as the filament protein EspA) to avoid confusion.

- EXPERIMENTAL MODEL AND STUDY PARTICIPANT DETAILS
  - Bacterial strains
  - Cell line culture
- METHOD DETAILS
  - Construction of plasmids expressing labeled EspB and TMD-exchanged EspB
  - Construction of a plasmid over-expressing EspD
  - EspB and EspD purification
  - Size exclusion chromatography (SEC)
  - SEC with multi-angle light scattering (MALS)
  - Translocation activity
  - Immunoblotting
  - *In vitro* type III secretion (T3S) assay
  - Pore-forming activity
  - Circular dichroism (CD) spectroscopy
- QUANTIFICATION AND STATISTICAL ANALYSIS
  - Statistical analysis

SUPPLEMENTAL INFORMATION

Supplemental information can be found online at https://doi.org/10.1016/j.isci.2024.109108.

ACKNOWLEDGMENTS

We thank Dr. Mario Lebendiker and Dr. Hadar Amartely from the Protein purification facility at the Hebrew University of Jerusalem, Israel, for assistance with the SEC-MALS analysis and Dr. B. Brett Finlay (University of British Columbia) and Dr. Rebekah DeVinney (University of Calgary) for antibodies against EPEC T3SS proteins.

Funding details: This work was supported by Israel Science Foundation research grant No. 988/19 to N.S.M.

AUTHOR CONTRIBUTIONS

J.G. and N.S.-M. designed the study, J.G, M.M., and I.R. performed the experiments and analyzed the data, J.E. conceived and designed the graphical model, J.G., M.M., I.R., J.E., and N.S.-M. drafted the manuscript. All authors made substantial and direct contributions to the work and approved the final version of the manuscript.

DECLARATION OF INTERESTS

The authors declare no competing interests.

Received: August 23, 2023
Revised: December 17, 2023
Accepted: January 31, 2024
Published: February 3, 2024

REFERENCES

1. Bergeron, J.R.C., and Marlovits, T.C. (2022). Cryo-EM of the injectisome and type III secretion systems. Curr. Opin. Struct. Biol. *75*, 102403. https://doi.org/10.1016/j.sbi.2022.102403.
2. Büttner, D. (2012). Protein export according to schedule: architecture, assembly, and regulation of type III secretion systems from plant- and animal-pathogenic bacteria. Microbiol. Mol. Biol. Rev. *76*, 262–310. https://doi.org/10.1128/MMBR.05017-11.
3. Cornelis, G.R. (2010). The type III secretion injectisome, a complex nanomachine for intracellular 'toxin' delivery. Biol. Chem. *391*, 745–751. https://doi.org/10.1515/BC.2010.079.
4. Deng, W., Marshall, N.C., Rowland, J.L., McCoy, J.M., Worrall, L.J., Santos, A.S., Strynadka, N.C.J., and Finlay, B.B. (2017). Assembly, structure, function and regulation of type III secretion systems. Nat. Rev. Microbiol. *15*, 323–337. https://doi.org/10.1038/nrmicro.2017.20.
5. Wagner, S., Grin, I., Malmsheimer, S., Singh, N., Torres-Vargas, C.E., and Westerhausen, S. (2018). Bacterial type III secretion systems: a complex device for the delivery of bacterial effector proteins into eukaryotic host cells. FEMS Microbiol. Lett. *365*, fny201. https://doi.org/10.1093/femsle/fny201.
6. Dey, S., Chakravarty, A., Guha Biswas, P., and De Guzman, R.N. (2019). The type III secretion system needle, tip, and translocon. Protein Sci. *28*, 1582–1593. https://doi.org/10.1002/pro.3682.
7. Luo, W., and Donnenberg, M.S. (2006). Analysis of the function of enteropathogenic *Escherichia coli* EspB by random mutagenesis. Infect. Immun. *74*, 810–820. https://doi.org/10.1128/IAI.74.2.810-820.2006.
8. Luo, W., and Donnenberg, M.S. (2011). Interactions and predicted host membrane topology of the enteropathogenic *Escherichia coli* translocator protein EspB. J. Bacteriol. *193*, 2972–2980. https://doi.org/10.1128/JB.00153-11.
9. Matteï, P.J., Faudry, E., Job, V., Izoré, T., Attree, I., and Dessen, A. (2011). Membrane targeting and pore formation by the type III secretion system translocon. FEBS J. *278*, 414–426. https://doi.org/10.1111/j.1742-4658.2010.07974.x.
10. Diepold, A., and Wagner, S. (2014). Assembly of the bacterial type III secretion machinery. FEMS Microbiol. Rev. *38*, 802–822. https://doi.org/10.1111/1574-6976.12061.
11. Notti, R.Q., and Stebbins, C.E. (2016). The Structure and Function of Type III Secretion Systems. Microbiol. Spectr. *4*. https://doi.org/10.1128/microbiolspec.VMBF-0004-2015.

12. Epler, C.R., Dickenson, N.E., Olive, A.J., Picking, W.L., and Picking, W.D. (2009). Liposomes recruit IpaC to the *Shigella flexneri* type III secretion apparatus needle as a final step in secretion induction. Infect. Immun. *77*, 2754–2761. https://doi.org/10.1128/IAI.00190-09.
13. Espina, M., Olive, A.J., Kenjale, R., Moore, D.S., Ausar, S.F., Kaminski, R.W., Oaks, E.V., Middaugh, C.R., Picking, W.D., and Picking, W.L. (2006). IpaD localizes to the tip of the type III secretion system needle of *Shigella flexneri*. Infect. Immun. *74*, 4391–4400. https://doi.org/10.1128/IAI.00440-06.
14. Bârzu, S., Benjelloun-Touimi, Z., Phalipon, A., Sansonetti, P., and Parsot, C. (1997). Functional analysis of the *Shigella flexneri* IpaC invasin by insertional mutagenesis. Infect. Immun. *65*, 1599–1605. https://doi.org/10.1128/iai.65.5.1599-1605.1997.
15. Collazo, C.M., and Galán, J.E. (1997). The invasion-associated type III system of *Salmonella typhimurium* directs the translocation of Sip proteins into the host cell. Mol. Microbiol. *24*, 747–756. https://doi.org/10.1046/j.1365-2958.1997.3781740.x.
16. Deng, W., Puente, J.L., Gruenheid, S., Li, Y., Vallance, B.A., Vázquez, A., Barba, J., Ibarra, J.A., O'Donnell, P., Metalnikov, P., et al. (2004). Dissecting virulence: systematic and functional analyses of a pathogenicity island. Proc. Natl. Acad. Sci. USA *101*, 3597–3602. https://doi.org/10.1073/pnas.0400326101.
17. Håkansson, S., Schesser, K., Persson, C., Galyov, E.E., Rosqvist, R., Homblé, F., and Wolf-Watz, H. (1996). The YopB protein of *Yersinia pseudotuberculosis* is essential for the translocation of Yop effector proteins across the target cell plasma membrane and displays a contact-dependent membrane disrupting activity. EMBO J. *15*, 5812–5823.
18. Kresse, A.U., Rohde, M., and Guzmán, C.A. (1999). The EspD protein of enterohemorrhagic *Escherichia coli* is required for the formation of bacterial surface appendages and is incorporated in the cytoplasmic membranes of target cells. Infect. Immun. *67*, 4834–4842. https://doi.org/10.1128/IAI.67.9.4834-4842.1999.
19. Lai, L.C., Wainwright, L.A., Stone, K.D., and Donnenberg, M.S. (1997). A third secreted protein that is encoded by the enteropathogenic *Escherichia coli* pathogenicity island is required for transduction of signals and for attaching and effacing activities in host cells. Infect. Immun. *65*, 2211–2217. https://doi.org/10.1128/iai.65.6.2211-2217.1997.
20. Krampen, L., Malmsheimer, S., Grin, I., Trunk, T., Lührmann, A., de Gier, J.W., and Wagner, S. (2018). Revealing the mechanisms of membrane protein export by virulence-associated bacterial secretion systems. Nat. Commun. *9*, 3467. https://doi.org/10.1038/s41467-018-05969-w.
21. Akeda, Y., and Galán, J.E. (2005). Chaperone release and unfolding of substrates in type III secretion. Nature *437*, 911–915. https://doi.org/10.1038/nature03992.
22. Allison, S.E., Tuinema, B.R., Everson, E.S., Sugiman-Marangos, S., Zhang, K., Junop, M.S., and Coombes, B.K. (2014). Identification of the docking site between a type III secretion system ATPase and a chaperone for effector cargo. J. Biol. Chem. *289*, 23734–23744. https://doi.org/10.1074/jbc.M114.578476.
23. Burkinshaw, B.J., and Strynadka, N.C.J. (2014). Assembly and structure of the T3SS. Biochim. Biophys. Acta *1843*, 1649–1663. https://doi.org/10.1016/j.bbamcr.2014.01.035.
24. Lunelli, M., Lokareddy, R.K., Zychlinsky, A., and Kolbe, M. (2009). IpaB-IpgC interaction defines binding motif for type III secretion translocator. Proc. Natl. Acad. Sci. USA *106*, 9661–9666. https://doi.org/10.1073/pnas.0812900106.
25. Faudry, E., Job, V., Dessen, A., Attree, I., and Forge, V. (2007). Type III secretion system translocator has a molten globule conformation both in its free and chaperone-bound forms. FEBS J. *274*, 3601–3610. https://doi.org/10.1111/j.1742-4658.2007.05893.x.
26. Montagner, C., Arquint, C., and Cornelis, G.R. (2011). Translocators YopB and YopD from *Yersinia enterocolitica* form a multimeric integral membrane complex in eukaryotic cell membranes. J. Bacteriol. *193*, 6923–6928. https://doi.org/10.1128/JB.05555-11.
27. Romano, F.B., Tang, Y., Rossi, K.C., Monopoli, K.R., Ross, J.L., and Heuck, A.P. (2016). Type 3 Secretion Translocators Spontaneously Assemble a Hexadecameric Transmembrane Complex. J. Biol. Chem. *291*, 6304–6315. https://doi.org/10.1074/jbc.M115.681031.
28. Croxen, M.A., and Finlay, B.B. (2010). Molecular mechanisms of Escherichia coli pathogenicity. Nat. Rev. Microbiol. *8*, 26–38. https://doi.org/10.1038/nrmicro2265.
29. Croxen, M.A., Law, R.J., Scholz, R., Keeney, K.M., Wlodarska, M., and Finlay, B.B. (2013). Recent advances in understanding enteric pathogenic *Escherichia coli*. Clin. Microbiol. Rev. *26*, 822–880. https://doi.org/10.1128/CMR.00022-13.
30. Ide, T., Laarmann, S., Greune, L., Schillers, H., Oberleithner, H., and Schmidt, M.A. (2001). Characterization of translocation pores inserted into plasma membranes by type III-secreted Esp proteins of enteropathogenic *Escherichia coli*. Cell Microbiol. *3*, 669–679. https://doi.org/10.1046/j.1462-5822.2001.00146.x.
31. Romano, F.B., Rossi, K.C., Savva, C.G., Holzenburg, A., Clerico, E.M., and Heuck, A.P. (2011). Efficient isolation of *Pseudomonas aeruginosa* type III secretion translocators and assembly of heteromeric transmembrane pores in model membranes. Biochemistry *50*, 7117–7131. https://doi.org/10.1021/bi200905x.
32. Schoehn, G., Di Guilmi, A.M., Lemaire, D., Attree, I., Weissenhorn, W., and Dessen, A. (2003). Oligomerization of type III secretion proteins PopB and PopD precedes pore formation in Pseudomonas. EMBO J. *22*, 4957–4967. https://doi.org/10.1093/emboj/cdg499.
33. Chatterjee, A., Caballero-Franco, C., Bakker, D., Totten, S., and Jardim, A. (2015). Pore-forming Activity of the Escherichia coli Type III Secretion System Protein EspD. J. Biol. Chem. *290*, 25579–25594. https://doi.org/10.1074/jbc.M115.648204.
34. Hutchison, J.M., Lu, Z., Li, G.C., Travis, B., Mittal, R., Deatherage, C.L., and Sanders, C.R. (2017). Dodecyl-beta-melibioside Detergent Micelles as a Medium for Membrane Proteins. Biochemistry *56*, 5481–5484. https://doi.org/10.1021/acs.biochem.7b00810.
35. Gershberg, J., Braverman, D., and Sal-Man, N. (2021). Transmembrane domains of type III-secreted proteins affect bacterial-host interactions in enteropathogenic *E. coli*. Virulence *12*, 902–917. https://doi.org/10.1080/21505594.2021.1898777.
36. Baruch, K., Gur-Arie, L., Nadler, C., Koby, S., Yerushalmi, G., Ben-Neriah, Y., Yogev, O., Shaulian, E., Guttman, C., Zarivach, R., and Rosenshine, I. (2011). Metalloprotease type III effectors that specifically cleave JNK and NF-κB. EMBO J. *30*, 221–231. https://doi.org/10.1038/emboj.2010.297.
37. Dickenson, N.E., Arizmendi, O., Patil, M.K., Toth, R.T., 4th, Middaugh, C.R., Picking, W.D., and Picking, W.L. (2013). N-terminus of IpaB provides a potential anchor to the Shigella type III secretion system tip complex protein IpaD. Biochemistry *52*, 8790–8799. https://doi.org/10.1021/bi400755f.
38. Guignot, J., Segura, A., and Tran Van Nhieu, G. (2015). The Serine Protease EspC from Enteropathogenic Escherichia coli Regulates Pore Formation and Cytotoxicity Mediated by the Type III Secretion System. PLoS Pathog. *11*, e1005013. https://doi.org/10.1371/journal.ppat.1005013.
39. Litvak, Y., Sharon, S., Hyams, M., Zhang, L., Kobi, S., Katsowich, N., Dishon, S., Nussbaum, G., Dong, N., Shao, F., and Rosenshine, I. (2017). Epithelial cells detect functional type III secretion system of enteropathogenic Escherichia coli through a novel NF-κB signaling pathway. PLoS Pathog. *13*, e1006472. https://doi.org/10.1371/journal.ppat.1006472.
40. Gauthier, A., Puente, J.L., and Finlay, B.B. (2003). Secretin of the enteropathogenic *Escherichia coli* type III secretion system requires components of the type III apparatus for assembly and localization. Infect. Immun. *71*, 3310–3319. https://doi.org/10.1128/IAI.71.6.3310-3319.2003.
41. Kaniga, K., Tucker, S., Trollinger, D., and Galán, J.E. (1995). Homologs of the *Shigella* IpaB and IpaC invasins are required for *Salmonella typhimurium* entry into cultured epithelial cells. J. Bacteriol. *177*, 3965–3971. https://doi.org/10.1128/jb.177.14.3965-3971.1995.
42. Ménard, R., Sansonetti, P., and Parsot, C. (1994). The secretion of the *Shigella flexneri* Ipa invasins is activated by epithelial cells and controlled by IpaB and IpaD. EMBO J. *13*, 5293–5302. https://doi.org/10.1002/j.1460-2075.1994.tb06863.x.
43. Faudry, E., Vernier, G., Neumann, E., Forge, V., and Attree, I. (2006). Synergistic pore formation by type III toxin translocators of Pseudomonas aeruginosa. Biochemistry *45*, 8117–8123. https://doi.org/10.1021/bi060452+.
44. Discola, K.F., Förster, A., Boulay, F., Simorre, J.P., Attree, I., Dessen, A., and Job, V. (2014). Membrane and chaperone recognition by the major translocator protein PopB of the type III secretion system of Pseudomonas aeruginosa. J. Biol. Chem. *289*, 3591–3601. https://doi.org/10.1074/jbc.M113.517920.
45. Myeni, S.K., Wang, L., and Zhou, D. (2013). SipB-SipC complex is essential for translocon formation. PLoS One *8*, e60499. https://doi.org/10.1371/journal.pone.0060499.
46. Tang, Y., Romano, F.B., Breña, M., and Heuck, A.P. (2018). The Pseudomonas aeruginosa type III secretion translocator PopB assists the insertion of the PopD translocator into host cell membranes. J. Biol. Chem. *293*, 8982–8993. https://doi.org/10.1074/jbc.RA118.002766.
47. Tardy, F., Homblé, F., Neyt, C., Wattiez, R., Cornelis, G.R., Ruysschaert, J.M., and Cabiaux, V. (1999). *Yersinia enterocolitica*

type III secretion-translocation system: channel formation by secreted Yops. EMBO J. *18*, 6793–6799. https://doi.org/10.1093/emboj/18.23.6793.

48. Godlee, C., and Holden, D.W. (2023). Transmembrane substrates of type three secretion system injectisomes. Microbiology (Read.) *169*, 001292. https://doi.org/10.1099/mic.0.001292.
49. Iguchi, A., Thomson, N.R., Ogura, Y., Saunders, D., Ooka, T., Henderson, I.R., Harris, D., Asadulghani, M., Kurokawa, K., Dean, P., et al. (2009). Complete genome sequence and comparative genome analysis of enteropathogenic *Escherichia coli* O127:H6 strain E2348/69. J. Bacteriol. *191*, 347–354. https://doi.org/10.1128/JB.01238-08.
50. Gibson, D.G., Benders, G.A., Andrews-Pfannkoch, C., Denisova, E.A., Baden-Tillson, H., Zaveri, J., Stockwell, T.B., Brownley, A., Thomas, D.W., Algire, M.A., et al. (2008). Complete chemical synthesis, assembly, and cloning of a Mycoplasma genitalium genome. Science *319*, 1215–1220. https://doi.org/10.1126/science.1151721.
51. Gibson, D.G., Young, L., Chuang, R.Y., Venter, J.C., Hutchison, C.A., 3rd, and Smith, H.O. (2009). Enzymatic assembly of DNA molecules up to several hundred kilobases. Nat. Methods *6*, 343–345. https://doi.org/10.1038/nmeth.1318.

STAR★METHODS

KEY RESOURCES TABLE

REAGENT or RESOURCE	SOURCE	IDENTIFIER
Antibodies		
Mouse anti-JNK	BD Pharmingen	Cat# Ab179461;RRID: AB_2744672
Mouse anti-actin	MPBio	Cat# 0869100-CF; RRID: AB_2920628
Mouse anti-EspB	Generously provided by Prof. B. Brett Finlay	NA
Rat anti-EspD	Generously provided by Prof. Rebekeh DeVinney	NA
HRP-goat anti-mouse	Abcam	Cat# Ab97040; RRID: AB_10698223
HRP-conjugated goat anti-rat	Jackson ImmunoResearch	Cat# Ab98425; RRID: AB_10675811
Bacterial strains		
Wild-type (WT) EPEC O127:H6 strain E2348/69 [streptomycin-resistant]	Iguchi et al.[49]	NA
EPEC Δ*escN* null mutant	Gauthier et al.[40]	NA
EPEC Δ*espB* null mutant	Luo and Donnenberg.[7]	NA
EPEC Δ*espD* null mutant	Lai et al.[19]	NA
E. coli DH10B	Thermo Scientific™	Cat# EC0113
Chemicals, peptides, and recombinant proteins		
Luria-Bertani (LB) broth	Toku-E	LB-LX-500
Streptomycin	Caisson Labs	S041-25GM
Carbenicillin	Formedium	CAR-0025
Nalidixic acid	Sigma-Aldrich	Cat# N8878
*Dpn*I	NEB	Cat# R0176S
Phusion	NEB	Cat# M0530L
Dulbecco's modified Eagle's medium (DMEM)	Gibco	Cat# 41965039
IPTG	Inalco	Cat# INA-1758-1400
Protease inhibitor cocktail	Roche	Cat# 5056489001
His Trap HP 1 mL columns	Cytiva	Cat# 17524701
Superose 12 10/300 GL column	GE Healthcare	Cat# 17-5173-01
Superdex 200 10/300 GL column	GE Healthcare	Cat# 17-5175-01
Superose 6 increase 10/300 GL	GE Healthcare	Cat# 29-0915-96
Imidazole	Sigma-Aldrich	Cat# I2399
Tween	Sigma-Aldrich	Cat# 8221840500
Coomassie	Abcam	Cat# Ab119211
DDM	Anatrace	Cat# D310
PMSF	Sigma-Aldrich	Cat# P7626
Nitrocellulose membrane (0.45 μm pore size)	Cytiva	Cat# 10-6000-02
PVDF membrane	Cytiva	Cat# 10-6000-23
0.22 μm filter	Millipore	Cat# SLGV033RS
Trichloroacetic acid (TCA)	Sigma-Aldrich	Cat# T0699
Propidium iodide (PI)	Sigma-Aldrich	Cat# P4170
Paraformaldehyde	EMS	Cat# 15710
Fetal Bovine Serum	Gibco	Cat# 10270-106

(*Continued on next page*)

Continued

REAGENT or RESOURCE	SOURCE	IDENTIFIER
Critical commercial assays		
EZ-ECL reagents	Cyanagen	Cat# XLS142,0250
BCA protein assay	Cyanagen	Cat# PRTD1.FS
Experimental models: Cell lines		
HeLa cell-line	CCL-2	ATCC
Oligonucleotides		
Primers used for cloning plasmids	See Table S2	NA
Recombinant DNA		
Plasmids used in this study	See Table S1	NA
Software and algorithms		
Adobe Illustrator	Adobe	https://www.adobe.com/
SnapGene	SnapGene	https://www.snapgene.com/
SPSS	IBM	SPSS statistics 29.0
ASTRA 6.1 software	Wyatt Technology	https://www.wyatt.com/library.html

RESOURCE AVAILABILITY

Lead contact

Further information and requiests can directed to Dr. Neta Sal-Man (salmanne@bgu.ac.il).

Materials availability

Strains and plasmids generated in this sutdy are available form the lead contact upon request.

Data and code availability

- All data reported in this paper will be shared by the lead contact upon request.
- This paper does not report any original code.
- Any additional information required to reanalyze the data reported in this paper is available from the lead contact upon request.

EXPERIMENTAL MODEL AND STUDY PARTICIPANT DETAILS

Bacterial strains

Wild-type (WT) EPEC O127:H6 strain E2348/69 [streptomycin-resistant][49] and EPEC null mutants (Δ*escN*, Δ*espB*, and Δ*espD*) were used to assess the T3SS and its translocation activities.[7,19,40] *E. coli* DH10B was used for plasmid handling. The *E. coli* strains (Table S1) were grown at 37°C in Luria-Bertani (LB) broth (Sigma) supplemented with the appropriate antibiotics. Antibiotics were used at the following concentrations: Streptomycin (50 μg/mL), carbenicillin (100 μg/mL), and nalidixic acid (50 μg/mL).

Cell line culture

HeLa (cervical carcinoma) cells were grown in DMEM supplemented with 10% FBS, 1% MEM, and 1% P/S at 37°C with 5% CO_2. The culture was passageed by splitting 1:10 twice per week. Cell suspensions were subsequently diluted to the desired cell density.

METHOD DETAILS

Construction of plasmids expressing labeled EspB and TMD-exchanged EspB

Cloning was performed using the Gibson assembly method.[50,51] The EspB protein was synthesized with a His_6-tag at position 36 to avoid disrupting its function. DNA encoding EspB amino acids 1–36 was amplified from EPEC genomic DNA using the primer pair EspB_Gib_F/EspB36_His_ R (the sequence of these and all other primers used in this study are listed in Table S2), which introduced a His_6-tag at position 36 of the EspB protein. In parallel, the fragment encoding the EspB protein starting from position 36 was amplified from EPEC genomic DNA using the primer pair EspB36_His_ F/EspB_notag_R. The two fragments were ligated using overlapping sequences and amplified using the primer pair EspB_Gib_F/EspB_notag_R. The pSA10 plasmid was amplified with the primer pair pSA10_F/pSA10_R. The PCR products were subjected to digestion with *Dpn*I, purified, and assembled by the Gibson assembly method. The resulting plasmid, $pEspB^{36}$-His (pSA10), translated into EspB bearing an internal His_6-tag at position 36.

The TMD-exchanged *espB* versions in the pSA10 plasmid were generated by amplifying the PCR fragment of Tir1+EspB$_{120-220}$, corresponding to the N-terminal TMD of Tir (Tir1) fused to the EspB sequence corresponding to amino acids 120–220, using the primer pair EspBTirTMDex1_F/EspB100aaTMD_R, with plasmid pEspB$_{Tir1}$-His (pSA10) as template.[35] Gibson assembly was conducted by amplifying the pEspB^{36}-His pSA10 vector with the primer pair EspB_TMD_open_F/EspB_TMD_open_R, followed by *Dpn*I treatment of the reaction products and subjecting the amplified vector and Tir1+EspB$_{120-220}$ to ligation. To generate plasmid pEspB^{36}-His Tir2, we used a similar design, only now amplifying the PCR fragment of Tir2+EspB$_{120-220}$, using the primer pair EspBTirTMDex2_F/EspB100aaTMD_R with plasmid pEspB$_{Tir2}$-His(pSA10) as template.[35] The resulting plasmids, pEspB^{36}-His Tir1 (pSA10) and pEspB^{36}-His Tir2 (pSA10), translated into EspB labeled with an internal His-tag at position 36 that contains either TMD1 or TMD2 of Tir instead of the original EspB TMD. All constructs were verified by DNA sequencing.

Construction of a plasmid over-expressing EspD

To clone an untagged version of EspD, DNA coding the *espD* sequenced was amplified from genomic DNA using the primer pair EspD_Gib_F/EspD_notag_R (Table S2). The pSA10 plasmid was amplified with the primer pair pSA10_F/pSA10_R. The PCR products were subjected to digestion with *Dpn*I, purified, and assembled by the Gibson assembly method. The resulting plasmid, pEspD$_{wt}$ (pSA10), was designed to over-express untagged EspD. The construct was verified by DNA sequencing.

EspB and EspD purification

EPEC Δ*espB* strain expressing EspB$_{wt}$-His, EspB^{36}-His, EspB^{36}-His Tir1, or EspB^{36}-His Tir1 were grown overnight in LB broth at 37°C with the appropriate antibiotics. The cultures were then diluted 1:50 in Dulbecco's modified Eagle's medium (DMEM, Biological Industries) and grown statically in a tissue culture incubator (37°C and 5% CO_2) for 3 h before adding 0.25 mM IPTG and grown for an additional 4 h. The cultures were centrifuged for 15 min at 12000 x *g*, and the supernatants containing the secreted EspB-His variants were collected. A protease inhibitor cocktail was added to the supernatants before being loaded onto His Trap HP 1 mL columns (GE Healthcare), washed with 50 mM imidazole, and eluted with 500 mM imidazole, according to the manufacturer's protocol. The eluted fractions were analyzed by SDS-PAGE and Coomassie staining to identify those fractions containing the purified proteins. A similar protocol was used to purify EspD^{35}-His from the supernatant of an EPEC Δ*espD* + pEspD^{35}-His culture (only with 1 mM IPTG) and to purify EspB^{36}-His from the supernatant of an EPEC Δ*espD* + EspB^{36}-His.

Size exclusion chromatography (SEC)

The purified EspB$_{wt}$-His sample was loaded onto a Superose 12 10/300 GL column (GE Healthcare) equilibrated in buffer containing 150 mM NaCl, 20 mM Tris-HCl pH 7.4 supplemented with or without 0.05% DDM and 0.5 mM PMSF at 4°C. The protein elution profile was monitored over time by UV detection. In addition, the EspB^{36}-His protein was loaded onto a Superdex 200 10/300 GL (GE Healthcare) equilibrated in buffer containing 150 mM NaCl, 20 mM Tris-HCl pH 7.4 or pH 4.5 supplemented with or without 0.05% DDM and 0.5 mM PMSF at 4°C. Purified EspD^{35}-His, EspB^{36}-His Tir1, and EspB^{36}-His Tir2 proteins were loaded onto a Superdex 200 10/300 GL (GE Healthcare) equilibrated in buffer containing 150 mM NaCl, 20 mM Tris-HCl pH 7.4 and 0.5 mM PMSF at 4°C. The void volume of the resin of this column under these conditions is 7.3 mL. Protein elution profiles were monitored over time by UV detection. Purified EspD^{35}-His sample was also loaded onto a Superose 6 10/300 GL column (GE Healthcare) equilibrated in buffer containing 150 mM NaCl, 20 mM Tris-HCl, pH 7.4, supplemented with 0.5 mM PMSF at 4°C. The void volume of the resin of this column under these conditions is 9.3 mL. Protein elution profiles were monitored over time by UV detection. Gel filtration standards comprising a mixture of molecular weight markers of known sizes were loaded onto the SEC columns. The volumes where the markers were eluted are indicated at the top of the SEC profiles.

SEC with multi-angle light scattering (MALS)

SEC-MALS measurements of EspB$_{wt}$-His were performed in a SEC-MALS system consisting of an AKTA Explorer (GE), MiniDawn TREOS multi-angle light scattering detector, and OPTILAB T-reX refractometer (Wyatt Technology, Santa Barbara, CA) set in-line with a size exclusion chromatography analytical column. A 400 µL aliquot of 0.45 mg/mL EspB$_{wt}$-His was applied to the apparatus. Experiments were performed using an AKTA PureM25 system with a UV-900 detector (GE) adapted for analytical runs. All experiments were performed at a elution rate 0.8 mL/min, with a running buffer comprising 20 mM Tris-HCl pH 7.4, 150 mM NaCl and 0.05% DDM. Detection was performed using three detectors measuring refractive index, ultraviolet absorption, and multi-angle laser-light scattering. Internal calibration was performed with monomer, dimer, and trimers of bovine serum albumin and cytochrome *c* proteins. Data collection and SEC-MALS analysis were performed with ASTRA 6.1 software (Wyatt Technology).

Translocation activity

Translocation assays were performed as previously described.[36] Briefly, HeLa cells (8 × 10^5 cells per well) were infected for 3 h with EPEC strains that were pre-induced for 3 h for T3SS activity (pre-heated DMEM, statically, in a CO_2 tissue culture incubator). Cells were then washed with PBS and lysed with RIPA buffer. Samples were centrifuged at maximum speed for 5 min to remove non-lysed cells, and supernatants were collected, mixed with SDS-PAGE sample buffer, and subjected to western blot analysis with anti-JNK and anti-actin antibodies (with actin serving as a loading control). Uninfected samples and the Δ*escN* mutant strain-infected samples served as negative controls.

Immunoblotting

Samples were separated by SDS-PAGE and electrotransferred to nitrocellulose (0.45 μm pore size; Bio-Rad) or PVDF (Mercury, Millipore) membranes. The membranes were blocked for 1 h using 5% (w/v) skim milk-PBST (0.1% Tween in phosphate-buffered saline), followed by incubation with primary antibodies. The primary antibodies were diluted in 5% skim milk-PBST and incubated at room temperature for 1 h or overnight at 4°C. Subsequently, the membranes were washed and incubated with secondary antibodies, diluted in 5% skim milk-PBST, and incubated for 1 h at room temperature. Chemiluminescence was detected using EZ-ECL reagents (Biological Industries). The primary antibodies used were mouse anti-JNK (BD Pharmingen), diluted 1:1000 in TBST, and mouse anti-actin (MPBio), diluted 1:10,000. Antibodies specific to T3SS components, including mouse anti-EspB and rat anti-EspD, were generously provided by Prof. B. Brett Finlay (University of British Columbia, Canada) and Prof. Rebekeh DeVinney (University of Calgary, Canada). Horseradish peroxidase-conjugated (HRP)-goat anti-mouse (Abcam) and HRP-conjugated goat anti-rat (Jackson ImmunoResearch) antibodies were used as secondary antibodies.

In vitro type III secretion (T3S) assay

EPEC strains were grown overnight in LB supplemented with the appropriate antibiotics in a shaker at 37°C. The cultures were then diluted 1:40 into pre-heated DMEM supplemented with the appropriate antibiotics and grown statically for 6 h in a tissue culture incubator (with 5% CO_2) to an optical density of 0.7 at 600 nm (OD_{600}). To induce protein expression, 0.5 mM IPTG was added after 2 h to the bacterial cultures. The cultures were then centrifuged at 20,000 × *g* for 5 min to separate the bacterial pellets from the supernatants. The pellets were dissolved in SDS-PAGE sample buffer, while the supernatants were collected and passed through a 0.22 μm filter (Millipore). The supernatants were then precipitated with 10% (v/v) trichloroacetic acid (TCA) overnight at 4°C to concentrate proteins secreted into the culture medium. Supernatant volumes were normalized according to bacterial culture OD_{600} readings to ensure equal sample loading. The samples were then centrifuged at 18,000 × *g* for 30 min at 4°C, the precipitated secreted proteins were dissolved in SDS-PAGE sample buffer, and the residual TCA was neutralized with saturated Tris-base. Proteins were separated on 12% SDS-PAGE gels and stained with Coomassie blue.

Pore-forming activity

Pore-forming activity was determined as previously described,[38,39] with slight modifications. Briefly, 5×10^4 HeLa cells were seeded per well of 96-well plates (black glass bottom plate, *In Vitro* Scientific). Upon reaching ~90% confluency, the cells were infected for 1.5 h at multiplicity of infection (MOI) of 1:100. The cells were then washed with cold PBS, incubated for 2 min with 3 mM propidium iodide (PI), washed twice, fixed with 4% paraformaldehyde and washed twice in PBS. PI uptake was measured by a plate reader (TECAN infinity 200pro, monochromators set at 533 nm excitation, 620 nm emission) and presented as relative fluorescence.

Circular dichroism (CD) spectroscopy

Samples of $EspB^{36}$-His, $EspB^{36}$-His Tir1, and $EspB^{36}$-His Tir2 proteins purified on Ni-NTA resin were added to dialysis tubes with a 3 kDa cutoff and incubated overnight in 10 mM sodium phosphate buffer at pH 7.5 to exchange the proteins samples into CD-suitable buffer. Spectra in the 190–260 nm range were recorded at room temperature on a Jasco J-715 spectropolarimeter (Tokyo) using a 1-mm quartz cuvette. Raw ellipticity is presented.

QUANTIFICATION AND STATISTICAL ANALYSIS

Statistical analysis

For statistical analysis, the IBM SPSS Statistics 29.0 package was used. An independent 2 tailed t-test with assumed equal variances was performed for the pore-forming assay. STD was used for error bars.